3.4 THE INTERACTION OF GRAVITY WAVES WITH TORNADOES AND MESOCYCLONES: THEORIES AND OBSERVATIONS

Timothy A. Coleman* and Kevin R. Knupp
The University of Alabama, Huntsville, Alabama

1. INTRODUCTION

Careful examination of Doppler radar data from several tornadic thunderstorms in Alabama and Tennessee reveals an intriguing yet strikingly consistent pattern. One or more relatively narrow bands of radar reflectivity approach a convective storm with a pre-existing mesocyclone, from its right flank (generally from a southerly direction). Then, upon interaction with the storm, there is an intensification of the mesocyclone and sometimes tornadogenesis. The reflectivity bands in these cases, however, can not generally be attributed to density currents/outflow boundaries from other storms, but instead appear to be gravity waves.

The interactions between gravity waves and *convection* have been well-investigated. Many have discussed the initiation or enhancement of convection by gravity waves (e.g., Uccellini 1975; Stobie et al. 1983; Corfidi 1998). Conversely, several others have shown that convective storms can also initiate gravity waves (e.g., Alexander et al. 1995; Bosart and Cussen 1973; Koch and O'handley 1997; Brunk 1949). The relationship known as wave-CISK, whereby convective lines and gravity waves synergistically support one another, has been well-examined also (e.g., Cram et al. 1992; Raymond 1984). However, the potential dynamic interactions between gravity waves and mesocyclones/tornadoes have received limited attention, and most of it has been observational in nature.

The occurrence of a Florida tornado on 14 November 1949 was related to the intersection of two "pressure jump lines" by Tepper (1950). In this case, one of the jump lines was apparently connected to a squall line, while the other may have been a gravity wave. Miller and Sanders (1980) observed that tornado production increased within some convective regions when wave packets overtook those regions during the Super Outbreak of April 1974. They posed a question in their paper as to whether or not the *waves contained vorticity which aided the development of tornadoes*. More recently, Kilduff (1999) observed the increase in storm rotational velocities and one case of tornadogenesis upon interaction with gravity waves on 22 January 1999 in northwest Alabama (a case to be studied in detail herein). Barker (2006) similarly finds a link between what he terms "reflectivity tags" moving quickly through a linear MCS and tornadogenesis, in the case of the F3 Evansville, Indiana tornado of 6 November 2005. These tags are likely gravity waves.

*Corresponding Author Address: Timothy A. Coleman, Atmospheric Science Department, The University of Alabama in Huntsville, 320 Sparkman Drive, Huntsville, AL 35805; Email: coleman@nsstc.uah.edu.

The purpose of this paper is to examine and model two physical processes which may help explain the gravity wave/mesocyclone interaction: 1) vortex stretching due to horizontal convergence associated with gravity waves, and 2) changing environmental wind shear due to wind perturbations within the waves. We will then examine these hypotheses in the context of two cases in which apparent gravity wave interactions with mesocyclones aided/initiated tornadogenesis. We will also briefly look at the wave/bore-like features which were related to a rapid intensification of the tornado (which was rated F5) in Birmingham, Alabama on 8 April 1998 (Pence and Peters 2000, Kilduff 1999).

2. BRIEF REVIEW OF WAVE DYNAMICS

Gravity waves may be excited when a parcel of air is perturbed vertically within an area of static stability. They may be initiated by convection, and also by other processes, including geostrophic adjustment, topography, and shear instability (Koch and O'Handley 1997). Gravity waves require some degree of static stability, but without a "duct" in place, wave energy would leak rapidly upward, preventing the maintenance of a coherent wave (Lindzen and Tung 1976). However, Lindzen and Tung (1976) showed that a wave may be "ducted" by a stable layer near the surface, as long as the stable layer 1) is deep enough to accommodate ¼ of the vertical wavelength, 2) contains no critical level, and 3) is topped by a conditionally unstable layer with a Richardson number Ri < 0.25. The *intrinsic* phase speed for a ducted wave is given by $c\text{-}U = 2ND\pi^{-1}$, where c is the ground-relative wave phase speed, U is the mean wave normal wind component in the duct, and D is the depth of the stable duct. Therefore, the phase speed may be determined through analysis of sounding data.

Eom (1975) developed a relatively simple model which simulates the gravity wave disturbance fairly well using a plane wave form, which may be written as $Q' = Q'_{max} \cos(kx-\omega t)$. Here, Q' may represent any of the perturbation variables in the gravity wave (ie., pressure p, wave relative perturbation wind u^*, and vertical motion w), and Q'_{max} would then represent the *amplitude* of each variable (as in Eom 1975). Also, k is the horizontal wavenumber, and ω is the angular frequency.

Such a wave is illustrated in Figure 1. The hydrostatically induced maximum p' (**H**) at the surface is co-located with the wave ridge (location of maximum upward displacement) and with u^*_{max} (as indicated by the wind vectors). Similarly, the minimum p' (**L**) is co-located with the wave trough and with $-u^*_{max}$. Low-level convergence ahead of the wave ridge produces upward

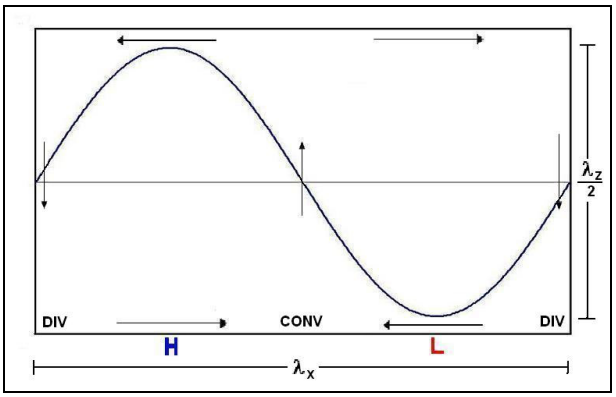

Figure 1. Idealized plane gravity wave (traveling to the right). Wind and vertical motion perturbations indicated by vectors, sinusoidal curve represents the displacement of an isentropic surface. (Adapted from Eom (1975); Bosart and Sanders (1986), and Cram et al. (1992).)

motion, and low-level divergence behind the ridge produces downward motion, allowing the ridge to propagate to the right.

It should be noted here that the highest likelihood for radar-detectable clouds and precipitation should logically be near or just ahead of the wave ridge. This is supported by the observations of Miller and Sanders (1980) and Sanders and Bosart (1985). So, a band of enhanced radar reflectivity would very nearly indicate the position of a gravity wave ridge.

3. DYNAMICS OF THE INTERACTIONS

3.1 *Convergence*

The vorticity equation (e.g. Holton 1992) states that the time rate of increase in vertical vorticity following the motion of a parcel is related to three processes: 1) stretching of pre-existing vorticity by horizontal convergence, 2) tilting of horizontal vorticity into the vertical, and 3) solenoidal effects. Typically, for mesoscale systems, we may neglect solenoidal effects.

For a plane gravity wave (as in Figure 1), convergence is maximized 90 deg ahead of the wave ridge. This convergence is significant in some cases. Time-to-space conversion of the Hytop, Alabama (HTX) WSR-88D VAD wind profile data (see Figure 2) of a mesoscale gravity wave in northeast Alabama on 10 May 2006 revealed convergence as large as 5 x 10^{-4} s^{-1}, which is consistent with the results found by Bosart and Seimon (1988). In the plane wave, the only horizontal wind perturbations are perpendicular to the wave front (ie., in the direction of wave motion). So, the stretching term of the vorticity equation for a wave may be written as

$$\frac{D\zeta}{Dt} = -\zeta \frac{\partial u^*}{\partial x} \qquad (1)$$

where x is taken as the direction of motion of the gravity wave. Convergence can not create vorticity where there is none, but it can enhance pre-existing vorticity. It may be shown mathematically, assuming the sinusoidal horizontal wind perturbation of the Eom (1975) model, that the increase in vorticity due to the passage of only *the convergent region* of a gravity wave is given by $\zeta_2 = \zeta_1 \exp(2u^*_{max}/c_R)$, where c_R is the phase speed relative to the mesocyclone motion. This makes physical sense, in that higher amplitude waves (larger u^*_{max}) produce larger vorticity changes, and slower moving waves (smaller c_R) have more time to act on the mesocyclone. For a typical mesoscale gravity wave, this indicates that the convergence ahead of the wave ridge may easily *double*, at least temporarily, the vorticity in a mesocyclone.

3.2 *Wind Shear*

Upon examination of the wind perturbations within a gravity wave (see Figure 1), it is clear that fairly significant perturbation wind shear may also accompany the wave, which significantly alters the environmental wind profile and storm-relative helicity. For the typical situation examined herein (a wave intersecting a rotating storm from its right flank), the wave trough region exhibits the perturbations which would typically enhance the vertical shear and the storm-relative helicity.

Consider the mesoscale gravity wave event of 10 May 2006 in northeast Alabama discussed above. The wave was moving ENE (from 250 deg) at 26 m s^{-1}, had a wave period of ~2 h, and its trough passed the HTX radar around 1945 UTC. VAD wind profiles in the lowest 10 kft (~3 km MSL) (Figure 2) show the winds within about ½ a vertical wavelength of the wave, similar to that illustrated in Figure 1. Note the extreme backing of the 2 kft winds (from 255 to 101 deg) between 1845 and 1945 UTC, associated with the *negative u** wind perturbations ahead of the trough. Also note the slight veering and considerable increase in magnitude of the winds at 10 kft (from 17 to 23 m s^{-1}), associated with the *positive u** perturbations near the ½ vertical wavelength height, as predicted by the model wave. A time-height section of the wave-normal wind field derived from this VAD profile is shown in Figure 3. There is a significant increase in wave-normal bulk shear in the layer shown, from 9.5 m s^{-1} at 1845 UTC, to 34.8 m s^{-1} at the wave trough (1945 UTC). This wave-induced shear has a significant effect on the helicity of the environment. Even in a ground-relative sense (as shown in the hodographs in Figure 4), the helicity increases dramatically within the wave trough (from near 0 at 1845 to ~150 m^2 s^{-2} at 1945 UTC), and considering that most examined cases have storms moving to the right of the

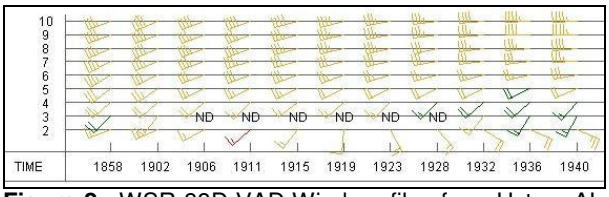

Figure 2. WSR-88D VAD Wind profiles from Hytop, AL (HTX) radar, 1858-1940 UTC, 10 May 2006.

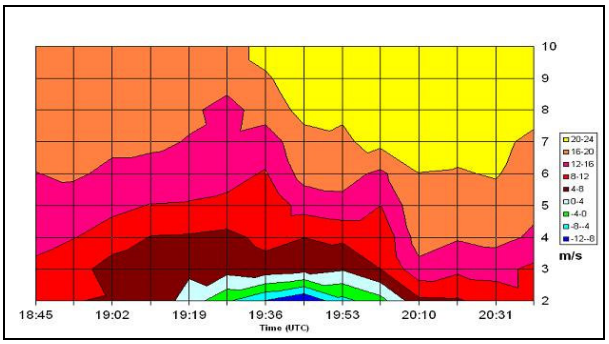

Figure 3. Time-height section of wave-normal wind magnitude, derived from HTX VAD wind profile data. Note surge of winds into the wave trough around its passage at 1945 UTC (10 May 2006).

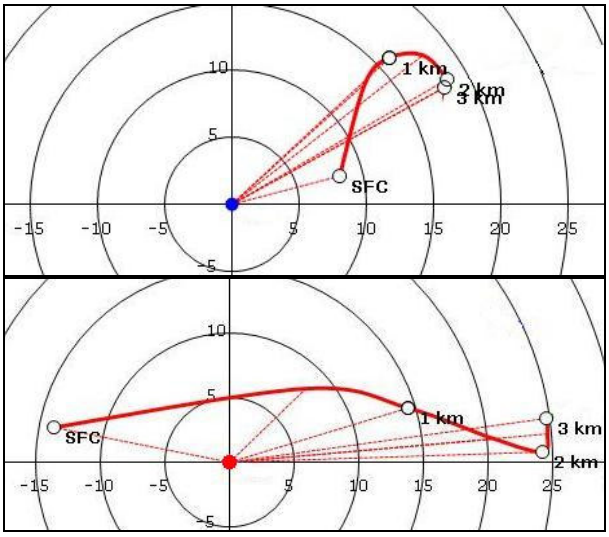

Figure 4. Hodographs of 0-3 km winds (m s^{-1}) derived from HTX VAD wind profile at 1845 UTC (top) and 1945 UTC (bottom) on 10 May 2006. Wind perturbations within the wave trough at 1945 UTC have significantly lengthened the hodograph and the ground-relative helicity.

wave vector, the storm-relative helicity should be higher.

The best way to examine the potential effect on a mesocyclone is to examine the tilting term in the vorticity equation, in a wave-normal coordinate system (as in section 3.1). It may then be written as:

$$\frac{D\zeta}{Dt} = \left(\frac{\partial u^*}{\partial z}\right)\left(\frac{\partial w}{\partial y}\right)\sin\alpha \qquad (2)$$

where w is vertical motion, x is in the direction of wave motion and y is orthogonal and to its left, and α is the angle between the wave vector and the mean storm-inflow in the wave layer. α must be considered, since we are attempting to isolate only the *streamwise* portion of the wave-induced horizontal vorticity, analogous to the storm-relative helicity.

3.3 *A combined numerical model*

A 2-dimensional numerical model was developed to simulate the interaction of a gravity wave with a pre-existing mesocyclone, utilizing equations (1) and (2) for the stretching and tilting processes, respectively. Now, there are so many variables involved, including (but not limited to) u^* and c, updraft strength w, and the relative orientation of the wave motion to the storm inflow, that a thorough treatment of even this simple model is beyond the scope of this paper.

However, the model will be applied here to a generic situation for discussion purposes. Suppose a storm containing a mesocyclone of initial vorticity 1 x10^{-2} s^{-1}, moving from 250 deg at 20 m s^{-1}, interacts with a gravity wave. For the wave, c=25 m s^{-1}, λ_x=50 km, its duct depth is 2000 m, and u^*_{MAX}=10 m s^{-1}. The model-simulated vorticity change with time is depicted in Figure 5. t=0 is taken as the time 90 deg ahead of the wave trough, and the model allows one full wavelength to pass the through the mesocyclone.

Throughout the first half of the wave, tilting due to enhanced shear is occurring. But, for the first ~200 s, the divergence ahead of the trough is strong enough to overcome the tilting and decrease the vorticity temporarily. But, after 200 s, the divergence weakens, and tilting overcomes it, allowing vorticity to begin to increase slowly. After trough passage, tilting is still occurring, but now convergence is occurring as well, ahead of the wave ridge. During the ¼ of the wave after the wave trough passes, *both tilting and stretching are acting at the same time*, and vorticity increases rapidly. Once the second half of the wave is passing, constructive tilting has stopped, but vorticity continues to increase slowly, reaching a peak > 5 x 10^{-2} s^{-1} just ahead of the wave ridge. So, this gravity wave has allowed a large increase in the vorticity within this mesocyclone, at least for a short period of time. As divergence takes back over after the ridge passes, the vorticity begins to decrease rapidly again, but perhaps

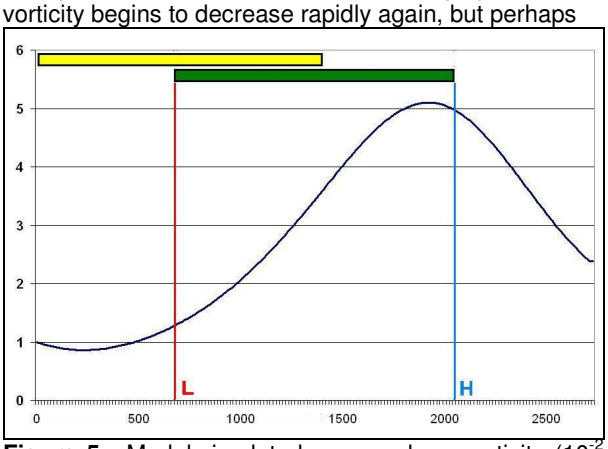

Figure 5. Model-simulated mesocyclone vorticity (10^{-2} s^{-1}) vs. time (s). **L** and **H** represent the wave trough and ridge passage, respectively. The yellow bar indicates the region of constructive vorticity tilting, and the green bar indicates positive vorticity stretching. The horizontal scale of the figure indicates a full horizontal wavelength.

most notably, *at the end of the full wavelength, the vorticity is still higher than it was initially, by a factor of more than 2!* As a matter of fact, if 2 identical waves with the parameters above interact with the mesocyclone, the vorticity reaches a maximum value ~ 7.5 x 10^{-2} s^{-1}, and a final value of 3.8 x 10^{-2} s^{-1}.

This is indeed a *fascinating preliminary result*, since one may expect variables affected by a periodic wave process to return to their original values after one full wavelength of the wave. But, this is not the case, indicating that the interaction is non-linear. Each gravity wave which interacts with a mesocyclone in the manner described above, produces a rather significant temporary increase in the vorticity, and a modest overall end-to-end increase as well. Simulations allowing t=0 to occur at various phases of the wave slightly altered the magnitude of the results, but the pattern in each case was essentially the same.

4. CASE STUDIES

4.1 *22 January 1999, Northwest Alabama*

On 22 January 1999, a rather stable but very high-shear environment existed over Alabama. The 1800 UTC sounding data from Birmingham (BMX) (see Figure 6) indicates that, above a shallow surface-based mixed layer, there is a rather deep stable layer, up to a height of about 1900 m MSL. A layer of lower static stability lies above 1900 m MSL.

Analysis of this sounding data according to the ducting parameters of Lindzen and Tung (1976), using the duct depth of 1732 m, and $N = 0.016$ s^{-1} indicate that this environment would support ducted gravity waves with phase speed c=37 m s^{-1}. Also, the synoptic-scale pattern, (e.g., Koch and O'Handley 1997), with a deep upper trough in the central part of the U.S., and a jet max apparently having rounded the base of

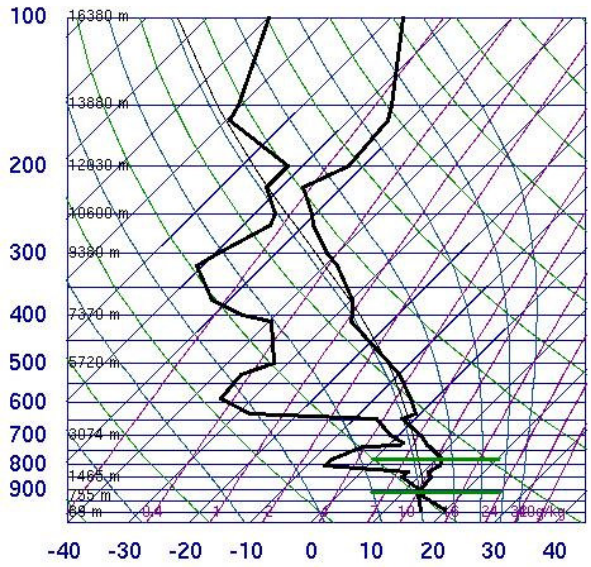

Figure 6. Skew-T, ln-p plot for sounding at BMX on 22 January 1999, 1800 UTC. Green lines show borders of stable layer which aides in ducting gravity waves.

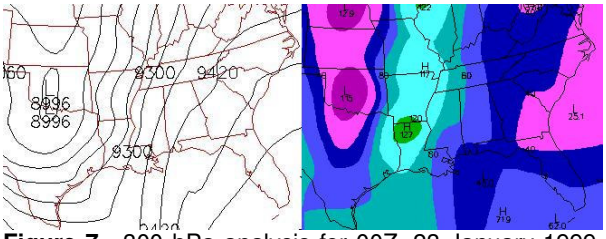

Figure 7. 300 hPa analysis for 00Z, 23 January 1999. Left panel shows heights (m), and right panel shows wind speed (kt). (Plymouth State Weather Center)

the 300 hPa trough during the day on 22 January 1999, provides a background favorable for wave generation through geostrophic adjustment (see Figure 7).

Rapidly developing severe convection moves into extreme western Alabama around 2000 UTC. Around the same time, a pair of mesoscale gravity waves appear on radar as two thin bands of enhanced reflectivity. These bands are classified as gravity waves, since the environment (synoptic and local) is favorable for their genesis and propagation, and since these bands are moving so rapidly northward at 32 m s^{-1}, which is fairly close to the predicted 37 m s^{-1}. It should be noted, too, that the air mass later in the day and farther west, closer to the incoming convection, could have been slightly more unstable, yielding lower phase speeds.

In Figure 8, one can clearly see an intense convective storm in Lamar County, AL (county on MS/AL state border), and one can also see the two apparent wave ridges. At the time of this image (2042 UTC), the initial wave ridge has just passed the mesocyclone, and the second wave, which appears more vigorous based on its radar reflectivity, is approaching the storm from the south. The second wave ridge intersects the mesocyclone at 2102 UTC, and the vorticity increases rapidly in the minutes just ahead of the wave ridge, as shown in Figure 9, reaching almost 2 x 10^{-2} s^{-1}. Shortly after 2102 UTC, a small tornado touched down in northern Fayette County,

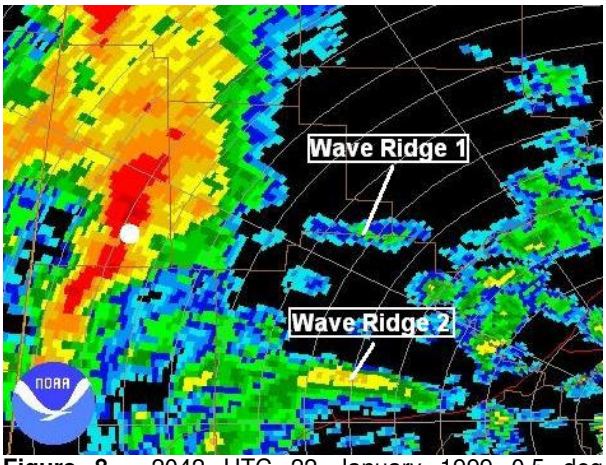

Figure 8. 2042 UTC 22 January 1999 0.5 deg reflectivity from WSR-88D radar at Birmingham, AL (BMX). White dot shows mesocyclone location.

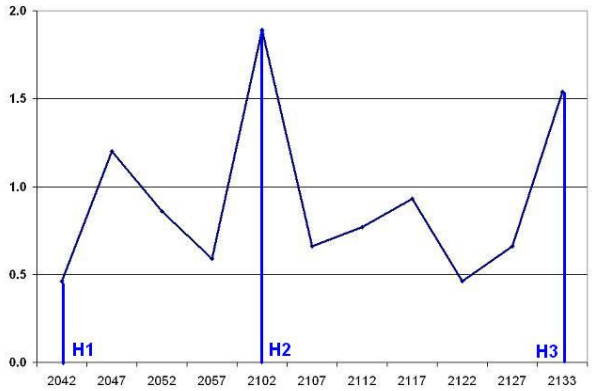

Figure 9. Vorticity (10-2 s-1) vs. time (UTC) for the northwest Alabama mesocyclone, 22 January 1999. Derived from BMX WSR-88D velocity data. H1, H2, and H3 indicate interaction times of mesocyclone with wave ridges.

Figure 10. 2102 UTC 0.5 deg storm-relative velocity (BMX) showing gate-to-gate maximized (magnitude > 50 kt, > 25 m s^{-1}) inbound and outbound velocities.

Alabama (the county containing the mesocyclone) (Kilduff 1999). The gate-to-gate, extreme wind shear in the mesocyclone at 2102 is shown clearly in Figure 10.

4.2 *16 December 2000, Tuscaloosa, Alabama*

At 1254 pm CST (1854 UTC) 16 December 2000, a tornado touched down in southwest Tuscaloosa County, on the west side of the Warrior River, to the east of I-20/59. This tornado, rated F4 on the Fujita scale, stayed on the ground over an 18 mile track, causing 11 fatalities and 75 injuries (NWS 2000).

The atmosphere was unseasonably unstable, with CAPE (using the 18 UTC sounding at nearby BMX) ~900 J kg^{-1}. Strong shear was present, with 0-6 km bulk shear of 18 m s^{-1} (35 kt). Despite the instability, there was a slightly stable ducting layer at low-levels, and the large wind shear probably also helped maintain wave coherence.

A supercell thunderstorm was already approaching Tuscaloosa (TCL) from the southwest at 1831 UTC. A band of reflectivity apparently associated with a gravity wave ridge approaches from the south (wave movement was from 200 deg at 32 m s^{-1}). It is again deduced that the band on radar is indicative of a gravity wave, since there is no convection to the south capable of generating an outflow boundary in this region, and the band is moving at 32 m s^{-1}, very close to the predicted wave speed of 30.2 m s^{-1}, utilizing the Lindzen and Tung (1976) duct equation with N=0.0098, D=1559 m.

As the area ahead of the apparent wave ridge(s) interacts with the storm, its mesocyclone intensifies, and the storm develops a reflectivity appendage on the southwest flank by 1852 UTC. Tornado touchdown occurs at 1854 UTC, indicating again that the apparent gravity wave may have played a role in tornadogenesis.

4.3 *8 April 1998, Birmingham, Alabama*

On 8 April 1998, beginning around 7:52 pm CDT, an F5 tornado moved through parts of eastern Tuscaloosa and western Jefferson counties (in Alabama), including some of the western suburbs of Birmingham. With this tornado, there were 32 fatalities and 258 injuries (Pence and Peters 2000). Though detailed discussion of this case will be deferred to later papers, it is worth noting here because the supercell was interacting with two or more parallel bands of enhanced reflectivity on radar, which could be wave-like undular bores, or gravity waves. In any event, upon interaction with one of these reflectivity bands (around 0058 UTC), a tornado that was already on the ground producing a narrow path of F0 damage, quickly intensified to F3, and the damage path became 1 km wide (Pence and Peters 1998). See Figure 11.

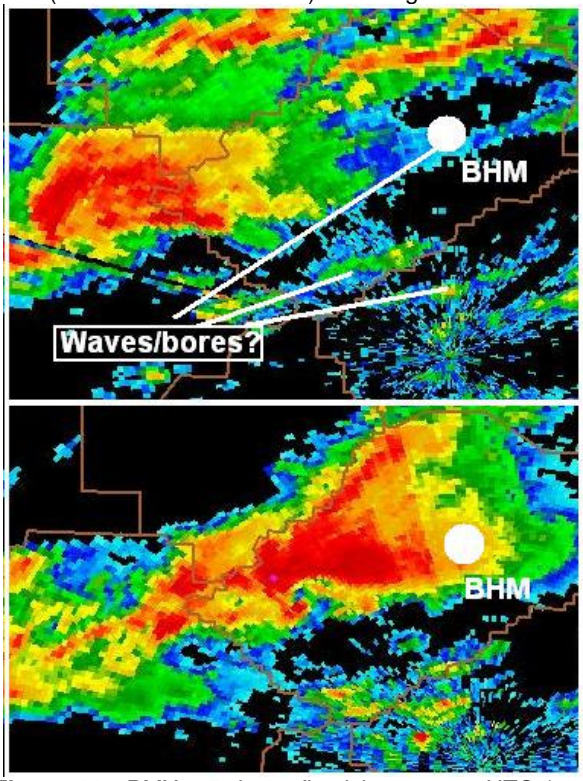

Figure 11. BMX 0.5 deg reflectivity at 0032 UTC (top) and 0103 UTC (bottom).

5. CONCLUSIONS

It is clear, not only through theoretical and numerical modeling considerations, but also through observations, that gravity waves may significantly impact mesocyclones/tornadoes with which they interact. The wind perturbations within the wave alter the environmental wind shear, and through tilting allow vorticity to be produced in the mesocyclone, while the convergence ahead of the wave trough helps to concentrate that vorticity through stretching.

The numerical modeling results herein produce an unexpected result: the response of a vortex (in this case a mesocyclone) to gravity waves is not simply periodic, but instead non-linear. Independent of which part of the wave interacts with the vortex first, after one full wavelength of interaction the *vorticity is always higher than it began*. Perhaps the vortex is somehow extracting energy from the wave, almost the opposite of a process, described by Chimonas and Hauser (1997), in which mesoscale vortices may *lose rotation energy to the environment* through gravity-swirl waves. This process must be examined much more closely.

In addition to more thorough examinations and 3-D numerical simulations of the cases presented, other cases of possible gravity wave/mesocyclone interaction also remain to be investigated, including the Nashville and Lawrenceburg (F5), Tennessee tornadoes of 16 April 1998. If this process can be better understood and introduced in the operational community, it could lead to better lead-time on tornado warnings, especially in low-CAPE, high-shear environments.

REFERENCES

Alexander, M. J., J. R. Holton, and D. R. Durran, 1995: The gravity wave response above deep convection in a squall line simulation. *J. Atmos. Sci.*, **52**, 2212-2226.

Barker, L. J., 2006: A potentially valuable WSR-88D severe storm pre-cursor signature in highly dynamic, low CAPE, high shear environments.

Bosart, L. F., and A. Seimon, 1988: A case study of an unusually intense atmospheric gravity wave. *Mon. Wea. Rev.,* **116,** 1857-1886.

Bosart, L. F., and F. Sanders, 1986: Mesoscale structure in the Megalopolitan snowstorm of 11-12 February 1983. Part III: A Large amplitude gravity wave. *J. Atmos. Sci.*, **43**, 924-939.

Bosart, L. F., and J. P. Cussen, 1973: Gravity wave phenomena accompanying East Coast cyclogenesis. *Mon. Wea. Rev.*, **101**, 446-454.

Brunk, I. W., 1949: The pressure pulsation of 11 April 1944. *J. Meteor.*, **6**, 181-187.

Chimonas, G., and H. M. Hauser, 1997: The transfer of angular momentum from vortices to gravity swirl waves. *J. Atmos. Sci.*, **54**, 1701-1711.

Corfidi, S. F., 1998: Some Thoughts on the role mesoscale features played in the 27 May 1997 central Texas tornado outbreak. *19th Conf. on Severe Local Storms*, American Meteorological Society.

Cram, J. M., R. A. Pielke, and W. R. Cotton, 1992: Numerical simulation and analysis of a prefrontal squall line. Part II: Propagation of the squall line as an internal gravity wave. *J. Atmos. Sci.*, **49**, 209-225.

Eom, J.-K., 1975: Analysis of the internal gravity wave occurrence of 19 April 1970 in the Midwest. *Mon. Wea. Rev.*, **103**, 217-226.

Holton, J. R., 1992: *An Introduction to Dynamic Meteorology*, 3rd ed.. Academic Press, 511 pp.

Kilduff, R. E., 1999: The interaction of a gravity wave with a thunderstorm. Electronic poster, NOAA/National Weather Service.

Koch, S. E., and C. O'handley 1997: Operational forecasting and detection of mesoscale gravity waves. *Wea. Forecasting*, **12**, 253-281.

Lindzen, R. S., and K. –K. Tung, 1976: Banded convective activity and ducted gravity waves. *Mon. Wea. Rev.*, **104**, 1602-1617.

Miller, D. A., and F. Sanders, 1980: Mesoscale conditions for the severe convection of 3 April 1974 in the East-Central United States. *J. Atmos. Sci.,* **37,** 1041-1055.

National Weather Service, 2000: Tuscaloosa Tornado, on-line storm report.

Pence, K. J., and B. E. Peters, 2000: The tornadic supercell of 8 April 1998 across Alabama and Georgia. *20th Conf. on Severe Local Storms,* American Meteorological Society.

Raymond, D. J., 1984: A wave-CISK model of squall lines. *J. Atmos. Sci.*, **41**, 1946-1958.

Sanders, F., and L. F. Bosart, 1985: Mesoscale structure in the Megalopolitan snowstorm, 11-12 February 1983. Part II: Doppler Radar Study of a New England snowband. *J. Atmos. Sci.*, **42,** 1398-1407.

Stobie, J. G., F. Einaudi, and L. W. Uccellini, 1983: A case study of gravity waves-convective storms interaction: 9 May 1979. *J. Atmos. Sci.*, **40**, 2804-2830.

Tepper, M., 1950: Radar and synoptic analysis of a tornado situation. *Mon. Wea. Rev.*, **78**, 170-176.

Uccellini, L. W., 1975: A case study of apparent gravity wave initiation of severe convective storms. *Mon. Wea. Rev.*, **103**, 497-513.